AN EXPERIMENTAL NUMERICAL PROCEDURE FOR REDUCING NOISE IN FORM-FEED ROTARY PRESSES

Andrea Bracciali, Monica Carfagni, and Paolo Citti
Dipartimento di Meccanica e Tecnologie Industriali
Università di Firenze - Via Santa Marta, 3 - 50139 Firenze, Italy

Paolo Rissone
Dipartimento di Energetica
Università de L'Aquila - 67040 Monteluco di Roio - L'Aquila, Italy

ABSTRACT: A combined numerical-experimental procedure for abating noise in rotary offset presses has been developed and testing. In the first stage, sound pressure and acceleration measurements were made on a test machine assembled in the laboratory. Two techniques, plate damping and structural modifications based on modal analysis, were combined to achieve reduction in the amplitude of the plate vibrations, found to be the major source of sound pressure.

1. INTRODUCTION

The international standards which define limits on noise emitted by machines in industrial plants reflect the growing concerns with the effects of noise on health and on output, especially where workers are subjected to high and/or prolonged sound pressure levels. Noise can thus be ranked along with cost, functionality, and performance as one of the major plant design factors. At the same time, as machines.grow increasingly lightweight and speedy, the problem of how to limit noise to acceptable levels is becoming more and more complex - to the extent that modern numerical and experimental techniques are being increasingly used to deal with noise abatement.

In this work, a combined noise abatement method is proposed for a rotary offset press that prints tractor-fed forms. Basically, there are two noise abatement methods: adding soundproof enclosures to acoustically isolate the machinery or acting upon the machinery and noise-producing mechanisms. We chose the second not only for the intrinsic advantage of built-in noise control, but also in view of the

fact that space-hogging enclosures would notably reduce the functionality of the presses, which necessitate frequent adjustment during operation.

2. DESCRIPTION OF THE TEST PRESS

The test rotary offset press prints tractor-fed forms such as invoices. The line comprises several units, each differing in type and function, which include a paper feeder, up to six different-color presses, a feed punch, and a form-fold and packaging unit.

The press rests on a rectangular base made of welded C-beams. The two lateral sides that support the cylinders for grinding, inking, and printing and their transmission devices are bolted to the base. The base is provided with housings for connecting the units.

Motion along the printing press line, which proceeds laterally and externally, is provided by Gleason bevel gears through a longitudinal shaft driven by an AC electric motor powered at variable current and frequency by an inverter. This system provides synchronization of the units (especially presses) and a variable output rate according to requirements, while respecting the technical limits of offset printing. Motion is transmitted by the bevel gear speed reducer to the printer unit by means of a preloaded toothed belt which provides dimensional independence and which filters out the feed's microirregularities.

The cylinders that receive motion from a set of cascaded gears protrude from the gear side of the press. Both the bearings and the gears are built to especially tight precision standards to ensure minimum clearances. This setup optimizes the machine's mechanical behavior and, in addition, serves to minimize noise from collision and sliding. Some cylinders, which have both rotational and translatory motion, are supported on hydrodynamic bearings and are driven by a crankshaft-rod mechanism. The shaft bearings and their supports are housed on the gearless (free) side of the machine. The two sides are connected by four bolted beams. These may be likened to trusses, since the connections, which have low connecting stiffness, act as hinges.

3. PRELIMINARY NOISE-CONTROL ANALYSIS

Testing was conducted in an actual rotary press plant to identify the main noise-emitting areas and to ascertain the real possibilities of abatement. The unit was moved to the laboratory to avoid the disturbances present in industrial settings. Since the setup differed considerably from the actual machine's, it was necessary to add a special motor featuring the specified speeds and adjustments (Figure 1). The unit was acoustically isolated so as not to disturb the sound pressure level measurements. The isolation enclosure was composed of a metal frame covered with 3-mm-thick lead plates internally lined with a cotton mattress, thereby ensuring excellent abatement over the whole frequency range. Testing was carried out at normal speed (main shaft rotating at 1500 rpm).

3.1. Sound Intensity Measurements

Sound intensity measurements were made over a range of 0 to 3200 Hz. Since the floor was assumed perfectly reflecting, only five measuring surfaces were used (Figure 1). Peaks are visible at the meshing frequencies of the Gleason stepdown gearing (500 Hz), of the gear train (600 Hz), and of the toothed gearbelt (450 Hz). It can be observed that the noise peaks do not coincide with any one gear, and that high levels are encountered all over the gear side.

As shown in Table I, approximately half of the total sound power is emitted at the paper input and output sides, with a difference between the gear and free sides of less than 2 dB.

TABLE I.   Sound intensity and sound power levels.

SIDE	SOUND INTENSITY LEVEL dB ref. 1E-12 W/m²	SOUND POWER LEVEL dB ref. 1E-12 W	W/Wtot (%)	AREA (m²)
GEAR	83.4	83.9	18	1.125
FREE	81.8	82.3	12	1.125
PAPER OUT	84.0	87.5	41	2.250
PAPER IN	79.7	82.2	12	1.800
TOP	85.0	83.6	17	0.720
TOTAL	83.0	91.4	100	7.020

3.2. Sound Pressure Level and Acceleration Measurements

Sound pressure and acceleration were measured between 0 and 800 Hz on the sides to determine the contribution of plate vibrations to overall noise. The markedly high values of the coherence function found at the meshing frequencies indicate a linear relation between the two. Plotted sound pressure and acceleration autospectra with their coherence function are shown in Figure 4. Note that the acceleration level rises 15 dB beyond 400 Hz.

3.3. Measurements at Varying Frequencies

The sound pressure and acceleration measurements were made at shaft rotating speeds varying between 500 and 1750 rpm. Figure 5 shows the sound pressure and acceleration waterfall spectra. It can be observed that several peaks change according to speed, since the exciting frequencies are linearly related to the shaft rotating speed, while those at the system's resonating frequencies do not reveal any change. Other peaks, multiples of 100 Hz, that do not correspond to any natural frequency, also remain unchanged, presumably because they depend on the harmonic couples introduced by the motor's electronic inverter.

4. PLATE MODELING

Sound pressure on the free side can be either airborne or generated by plate vibration. As intensity measurements show that the sound power only comes out of the free side, the airborne noise is evidently not a disturbing element.

The sound power emitted by a vibrating surface is

$$W = \delta \, c \, A \, \sigma_{rad} \, \langle v^2 \rangle \tag{1}$$

where

δ = air density (≈ 1.25 kg/m^3)

c = speed of sound in air (≈ 340 m/s)

A = area of radiating surface (m^2)

σ_{rad} = radiation efficiency ($0 < \sigma_{rad} \le 1$)

$\langle v^2 \rangle$ = space- and time-averaged mean square surface velocity

When the plates move stiffly, radiation efficiency may be assumed unitary; otherwise, if the sound is generated at frequencies near or the same as the structure's natural resonating frequencies, several parts of the plate will move counterphase in relation to the others, thereby possibly canceling out the adjacent sound ranges. In these cases, all other factors being equal, the radiation efficiency is less than one.

Recalling that $v = a / \omega$ and that $H(f) = a(f)/F(f)$, we can rewrite Equation (1)

$$W = \sigma \, c \, A \, \sigma_{rad} \, \langle (F*H)^2 \rangle / \omega^2 \tag{2}$$

Since (2) is expressed in the frequency range and not in the time range, the term $\langle (F*H)^2 \rangle$ relates to a point representing the motion of the structure.

Since the plates are rather thick, it can be assumed that the moving elements on the gear side are a source of dynamic excitation as well as of noise. The dynamic excitations cause the sides, which are efficient sound-emitting surfaces, to vibrate. They also explain the high sound power level found at the paper in and out sides: the sound generated inside the gap between the plates is not transmitted to the outside and sound reverberation causes self-excitation of the plates. Direct experimental verification of this phenomenon is obviously impossible, since measuring sound intensity inside the machine - impossible, on account of the cylinders - would entail reflections of such magnitude as to result unacceptable.

5. STRATEGIES TO REDUCE ACOUSTIC EMISSIONS

We have seen that the main source of sound pressure is plate vibration. To reduce the amplitude of the vibrations, we shall use two techniques, plate damping and modal analysis, to obtain the dual objective of shifting the resonance frequencies out of the excitation range and reducing the FRF amplitude in the excitation range.

5.1. Using Plate Damping To Reduce Acoustic Emissions

A simple model was developed to quantify the acoustic emissions of a metal plate excited by periodic sources such as the one acting on the unit. The model consisted of a suspended test plate mounting an excitation device comprising a three-phase AC electric motor and a cylinder double-stage stepdown gearing (Figure 6). The sound levels were measured inside a semianechoic room. Testing was carried out between 0 and 3200 Hz on four different setups:

Setup 1: Excitation device
Setup 2: Excitation device + one 15-mm plate
Setup 3: Excitation device + two 15-mm plates bolted together
Setup 4: Excitation device + two 15-mm plates taped with two-sided masking tape.

The excitation device, which rotated virtually unloaded since the stepdown gearing was not connected to any user, was mounted on a single plate to investigate the effect of the assembly on sound power level. To determine the effect of an increase in the thickness of the plate, a double plate was created by uniting two 15-mm plates to produce a 30-mm thickness equal to that of the actual machine. The plate's mass and stiffness were thus increased and damping due to the inevitable sliding between the two bending plates was introduced. The damping effect was increased by inserting a layer of two-sided masking tape in between the two 15-mm plates, thereby producing a constrained layer. Test results appear in Table II.

TABLE II. Measured sound power levels for the excitation unit alone and together with plates (all surfaces).

Setup #	Sound power level (dB ref. 1E-12 W)	Differences (dB)	
1 (excitation device alone)	70.3	ref.	——
2 (single 15-mm plate)	76.9	+6.6	ref.
3 (two bolted 15-mm plates)	75.6	+5.3	-1.3
4 (two taped 15-mm plates)	73.2	+2.9	-3.7

In further testing, performed with an instrumented hammer as the excitation device, the transfer functions were measured between the points shown in Figure 6. The FRF plots for cases 3 and 4 in Figure 7 both show a marked decrease in the peak amplitudes and an increase in damping.

Damping from the constrained layer was then examined as an aid in reducing acoustic emissions. To be successful, the constraining-plate thicknesses must be carefully chosen to provide a proper tradeoff between mass and flexural stiffness. For example, the selection of two plates of equal thickness can lead to an unacceptable decrease in flexural stiffness if the total thickness must be kept low. In the test case, thicknesses of 6 mm (constraining plate) and 1.2 mm (constrained layer damping material) were selected for damping a 30-mm-thick plate. The damping material, Diad 606, a polymer made specially

for these applications, was attached using a two-component epoxy glue (Araldit).

To get a more accurate understanding of the radiation properties of the acoustic noise source, measurements were also made on two new setups on the side opposite the excitation units:
Setup 5: Excitation device with one 30-mm plate
Setup 6: Excitation device with one 30-mm plate, one 1.2-mm Diad, and one 6-mm constraining plate.

Test results are shown in Table III.

TABLE III. Measured sound power levels for the excitation unit alone and together with plates (surface opposite motor).

Setup #	Sound power level (dB ref. 1E-12 W)	Differences (dB)		
1 (excitation device alone)	61.9	ref.	——	——
2 (single 15-mm plate)	70.2	+8.3	ref.	——
3 (two bolted 15-mm plates)	68.7	+6.8	-1.5	——
4 (two taped 15-mm plates)	65.0	+3.1	-5.7	——
5 (single 30-mm plate)	66.6	+4.7	-3.6	ref.
6 (two 30+1.2+6-mm plates)	63.1	+1.2	-7.1	-3.5

Note that the 30-mm plate with the Diad (Setup 6) revealed such high damping that no detectable signal could be discerned, thus making it impossible to measure the FRF.

5.2. Using Modal Analysis To Reduce Acoustic Emissions

The modal analysis procedure used to reduce acoustic emissions involves three steps:

Step 1: Obtaining the experimental modal model
Step 2: Simulating structural modifications
Step 3: Verifying structural modifications.

Step 1: Obtaining the Experimental Modal Model

An experimental modal analysis was carried out between 0 and 800 Hz to determine the vibratory behavior of the structure. Prior to testing, it was necessary to disassemble some of the inking rubber cylinders so that damping could be reduced to levels acceptable for testing. The structure was discretized into 44 degrees of freedom (DOFs) along the y axis, since, as could be expected, the principal motion was found to run along that axis. Test equipment consisted of a randomly excited permanent-magnet electromagnetic shaker as an excitation device, an impedance head to measure acting forces, and a magnetic-base piezoelectric accelerometer to measure acceleration. Signals were processed on a dual-channel FFT analyzer.

The resonance frequencies of the original (unmodified) structure

are shown in Table IV. It can be observed that several resonance frequencies exist in the excitation frequency range. After processing, the modal model was validated by synthesizing several frequency responses among the various pairs of machine points and verifying them experimentally.

Spectra of forces acting on the system, computed using the relation $F(f) = a(f)/H(f)$, highly excite the structure at the structure's own closely spaced modes (Figure 8). Force spectra values are amply qualitative, since the system has several inputs, and their partial coherence is most likely extremely high, since the excitations all arise from the same phenomena. Hence, what we actually did was to analyze the behavior of the structure under the effect of a force that incorporates all the others, thereby eliminating the need to remove the part linearly dependent on the others from each single force.

Step 2: Simulating Structural Modifications

Having obtained the experimental modal model, we could determine a set of feasible structural modifications. Structural modifications (Figure 9) were needed so as not to alter machine functionality. To reduce the plates' bending motion, simple 80 x 30-mm ribs were simulated horizontally and vertically at the plate ends using specially designed software. The resonance frequencies of the unmodified and modified structures are compared in Table IV.

TABLE IV. Comparison of the resonance frequencies of the unmodified and modified structures from 0 to 800 Hz.

Mode #	Unmodified structure			Modified structure		
	Freq(Hz)	Damp(%)	Damp (Hz)	Freq(Hz)	Damp(%)	Damp (Hz)
1	15.54	4.85	.76	100.15	.75	.76
2	58.33	3.18	1.85	118.66	1.56	1.85
3	63.53	2.52	1.60	166.68	.96	1.60
4	98.56	1.83	1.80	217.03	.83	1.80
5	116.42	4.01	4.68	268.62	1.74	4.78
6	166.59	4.96	8.28	317.81	2.60	8.28
7	261.07	3.82	9.98	400.03	2.49	9.98
8	309.39	1.23	3.80	672.63	.57	3.80
9	337.92	6.13	20.75	725.77	2.86	20.75
10	419.50	2.12	8.92			
11	479.50	2.16	10.38			
12	544.94	2.69	14.67			
13	647.67	2.34	15.19			.
14	673.17	1.17	7.84			
15	750.92	1.42	10.67			

Figure 10 shows the measured and postcalculation synthesized FRF 1Y/1Y (gear side upper left corner). The displacement of all the resonance frequencies upward allows easier damping. What is more, there is a marked decrease - of around 10 dB - in the amplitude of the FRF at the excitation frequencies (400 - 650 Hz). Assuming that the proposed structural modifications do not change the amplitude of forces

acting on the system - with meshing conditions left unchanged - accelerations and thus presumably the sound levels will be considerably reduced.

Step 3: Verifying Structural Modifications

Mathematical modeling of welded stiffeners has been experimentally validated (ref.1). In this case, as welding ribs to the sides of the machine proved technically impossible, we examined the feasibility of using screws, i.e., whether the connecting forces would be able to prevent contact sliding to ensure structural continuity.

A test model was built from a 30-mm-thick rectangular plate measuring 300 x 400 mm (Figure 11). Ribs with rectangular 30 x 80- mm sections of various lengths were assembled in several positions on the model using high-resistance M8 screws. Testing was carried out on the suspended plate using an impact hammer and was followed by simulation of the modifications. The test plate with the rib locations is illustrated in Figure 11.

Agreement of the calculated and experimental modal results was excellent in the frequency range under examination (0 - 2000 Hz). The resonance frequency with error percentages are shown in Table V. Calculated modal shapes very closely approximate experimental ones.

TABLE V. Comparison of experimental and calculated frequencies
for a stiffened plate with different rib location.

Free	Vertical rib Exp. Sim. Err.%			Horizontal rib Exp. Sim. Err.%			Diagonal rib Exp. Sim. Err.%		
778	730	681	-6.8	699	684	-2.1	860	816	-5.1
960	1204	1262	+4.8	810	879	+8.5	1309	1263	-3.5
1705	1329	1476	+11.0	1707	1669	-2.2	1712	1962	+14.6
1788	1937	1997	+3.1	1769	1864	+5.4	2171	2172	0.0

The simulated modal shape deflection for the diagonal rib's last frequency shows poor agreement with the experimental value, since too few DOFs were used to simulate attachment to the structure.

6. CONCLUSIONS

A combined numerical-experimental procedure for abating noise in rotary offset presses is described in this work. In laboratory testing, plate vibrations were found to be the major source of noise, which constrained-layer damping reduced by approximately 4 dB. By simulating structural modifications applied to an experimental modal model, it was also possible to estimate a drop of 10 dB in the plate acceleration level at the exciting frequencies. It is hoped that a forthcoming in-depth investigation will validate these preliminary results.

REFERENCES

(1) C. BRACCESI AND M. CARFAGNI, "Simulating Some Structural Dynamic Modifications through Experimental Modal Analysis," Bruel & Kjaer Technical Review, No. 1, 1988, p. 1-22.

(2) D.J. EWINS, Modal Testing: Theory and Practice, Bruel & Kjaer, 1986.

(3) S. TIMOSHENKO AND D.H. YOUNG, Vibration Problems in Engineering, Van Nostrand Reinhold, New York, New York, 1954.

(4) C. BRACCESI, M. CARFAGNI, AND P. RISSONE, "Using Vibratory and Modal Analysis To Reduce Vibration and Noise in an Automotive Engine," Proceedings, 6th IMAC, 1988, p. 973-979 and also in The International Journal of Analytical and Experimental Modal Analysis, Vol. 3, No. 3., July 1988, p. 89-95.

(5) M. CARFAGNI, P. RISSONE, AND M. SPEZIA, "Procedura di ottimizzazione strutturale di una macchina utensile dal punto di vista dinamico," Proceedings, 16th AIAS Congress, Ancona, Italy, 1988, p. 105-116.

(6) A. BRACCIALI, R. CAPITANI, AND M. CARFAGNI, "Caratterizzazione dinamica di un deviatoio ferroviario per alta velocità," Proceedings, 17th AIAS Congress, Ancona, Italy, 1989, p. 105-116.

(7) S.J. YANG AND A.J. ELLISON. Machinery Noise Measurements, Oxford University Press, Oxford, U.K., 1985.

(8) M.J. CROCKER AND F. M. KESSLER, Noise and Noise Control, Vol. 2, CRC Press, Boca Raton, Florida, 1982, p. 52-78.

(9) D.E. BAXA (editor), Noise Control in Internal Combustion Engines, John Wiley, New York, New York, 1982, p. 203-218 and 403-432.

(10) P.M. MORSE AND K.U. INGARD, Theoretical Acoustics, McGraw-Hill, New York, New York, 1986, p. 366-399.

(11) Handbook of Noise and Vibration Control, Trade and Technical Press Ltd., Morden, Surrey, U.K., 1983, p. 193-221.
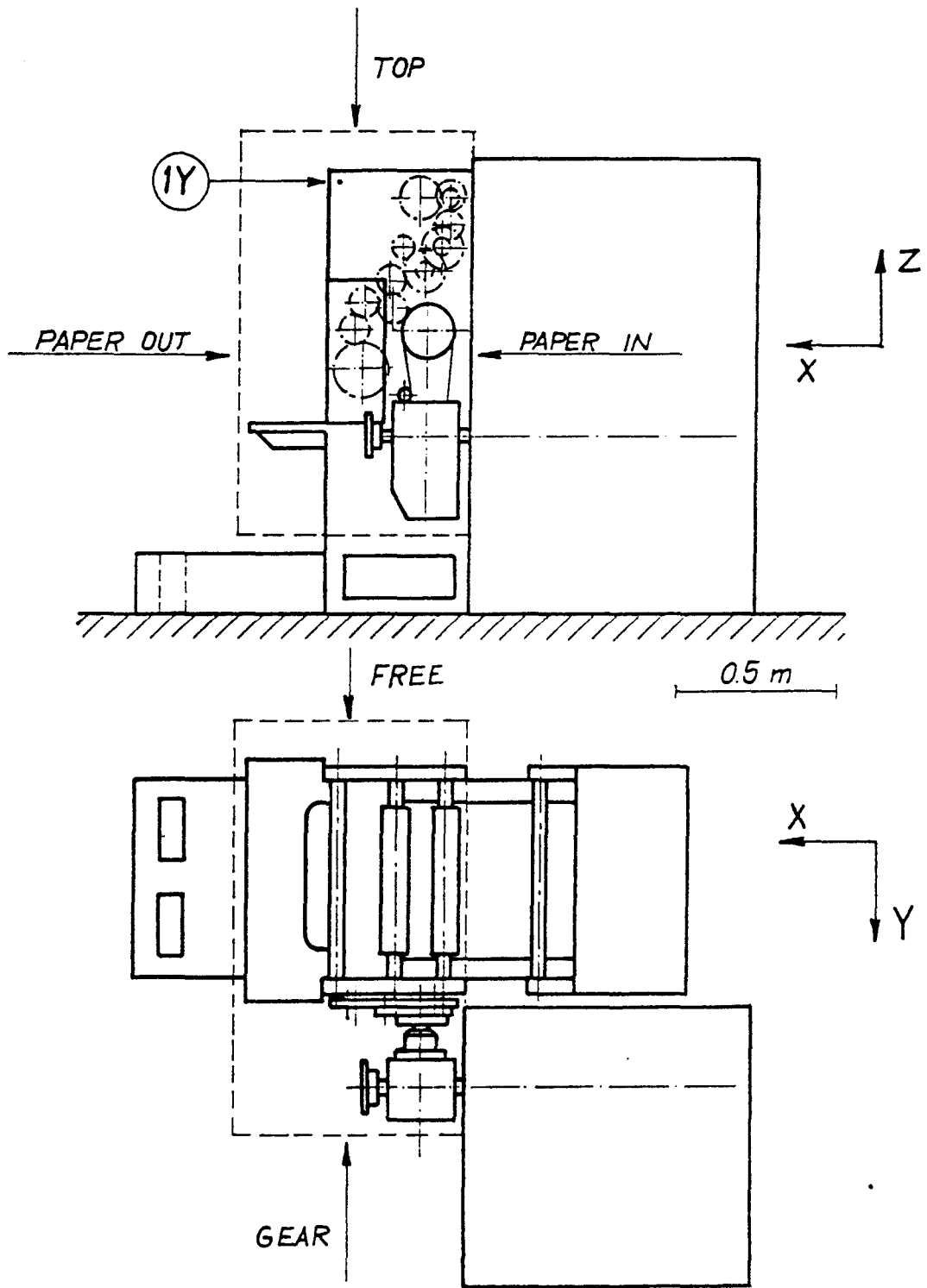
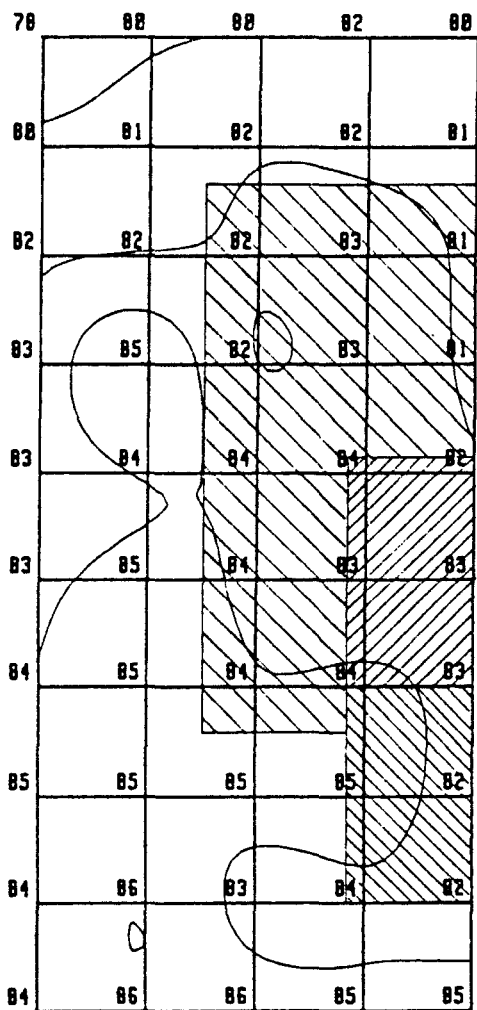Figure 1. Schematic of a form-feed rotary press.

78	88	88	82	88
88	81	82	82	81
82	82	82	83	81
83	85	82	83	81
83	84	84	84	82
83	85	84	83	83
84	85	84	84	83
85	85	85	85	82
84	86	83	84	82
84	86	86	85	85

81	88	79	79	78
88	88	79	78	76
88	88	88	78	81
81	81	88	81	81
83	83	82	79	83
83	83	83	81	81
82	83	81	81	81
83	83	84	82	83
81	82	84	82	84
84	84	82	84	85

GEAR TRAIN

TOOTHED BELT

BEVEL GEAR

Figure 2. Sound intensity map
of gear side.
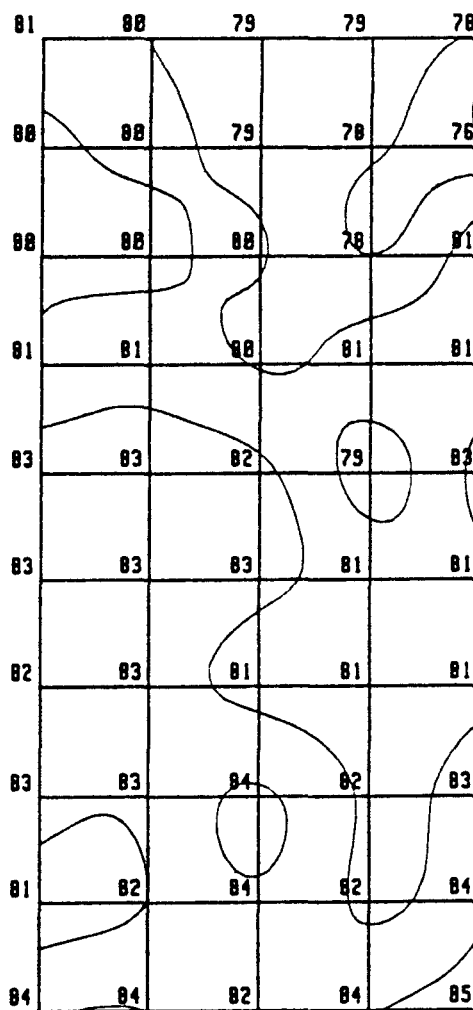
Figure 3. Sound intensity map
of free side.
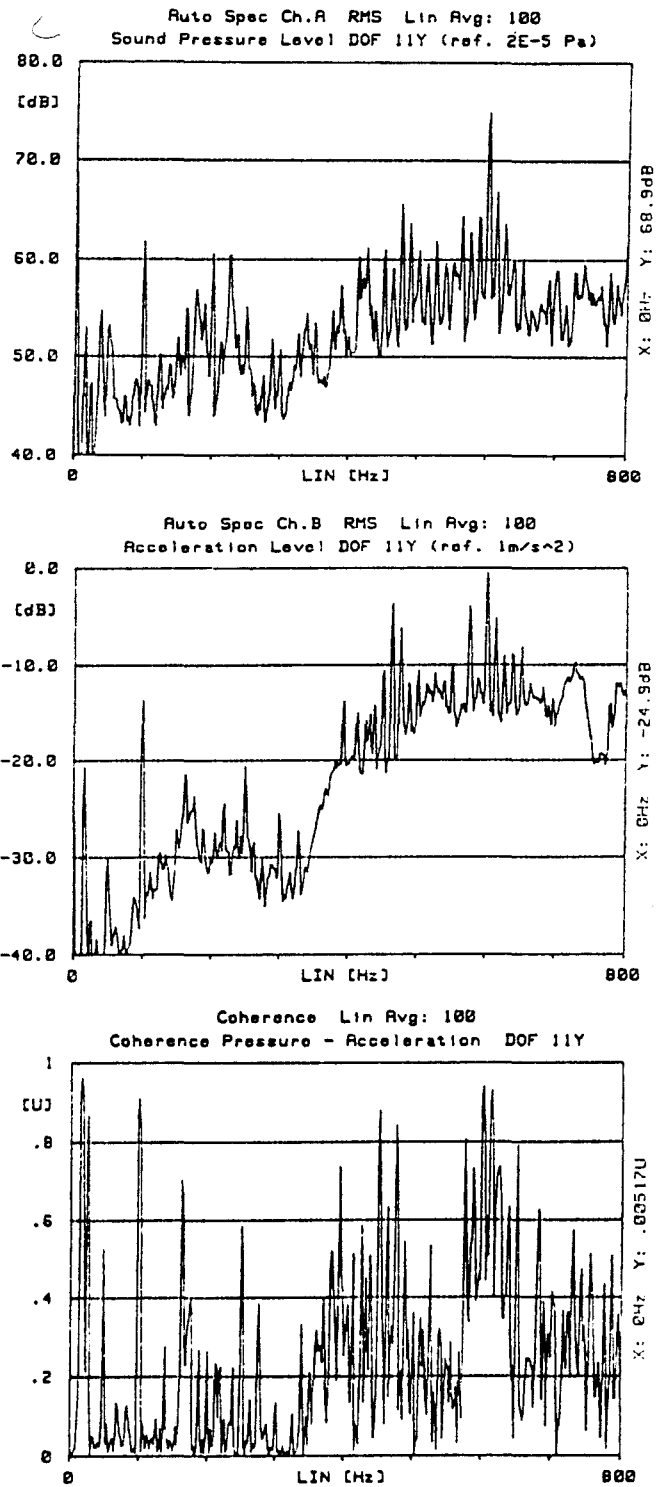
Figure 4. Sound pressure and acceleration autospectra (top and middle); coherence function (bottom).
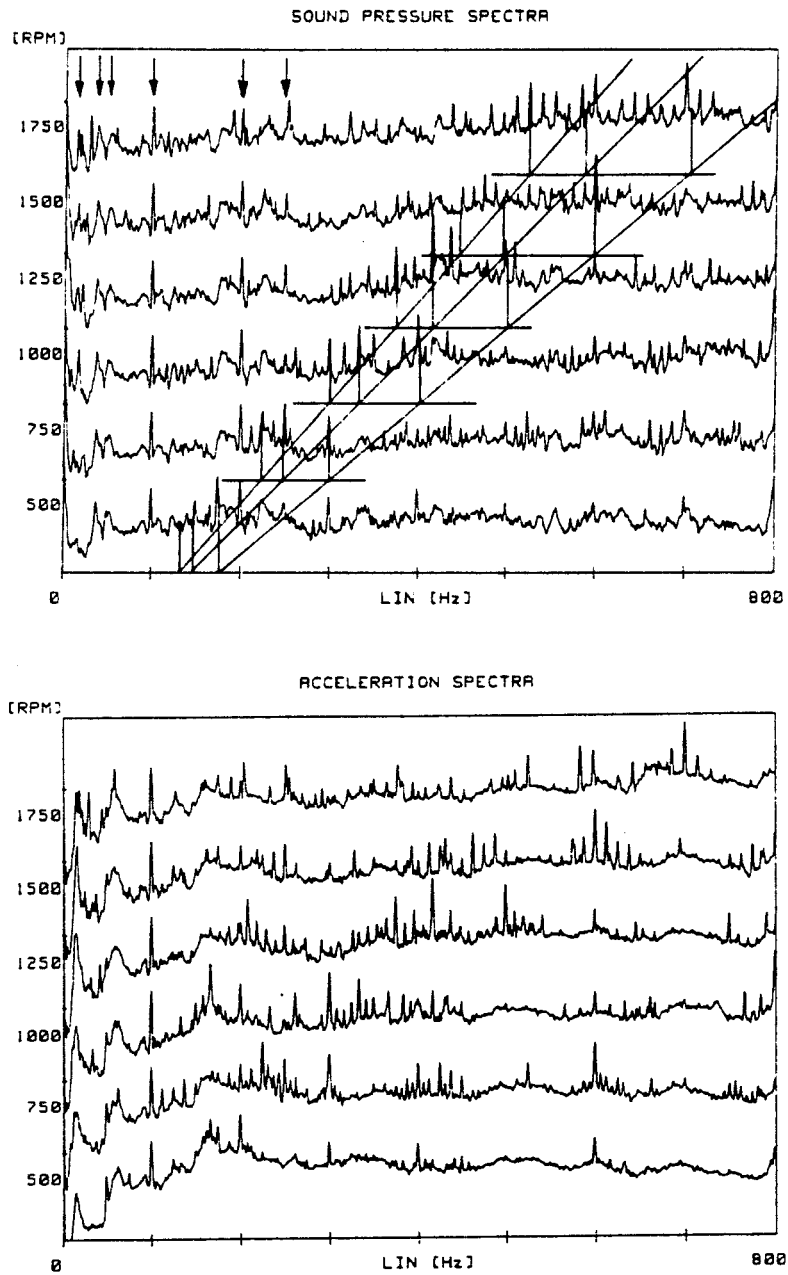
Figure 5. Sound pressure and acceleration waterfall diagrams.
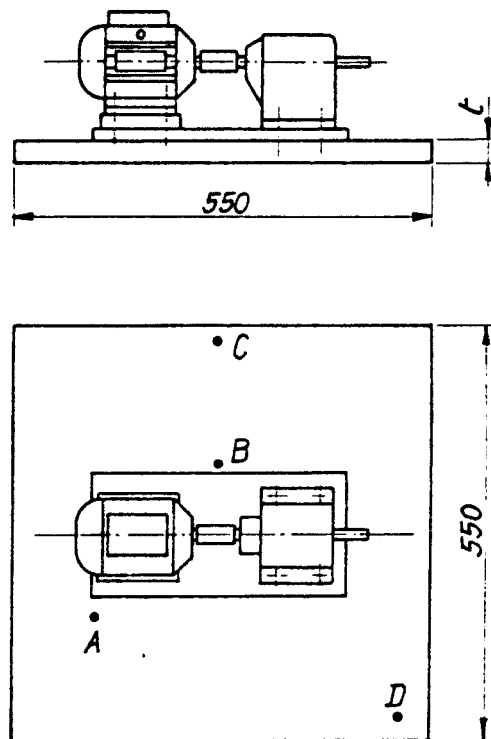
Figure 6.   Schematic of excitation device for measuring sound   emitted
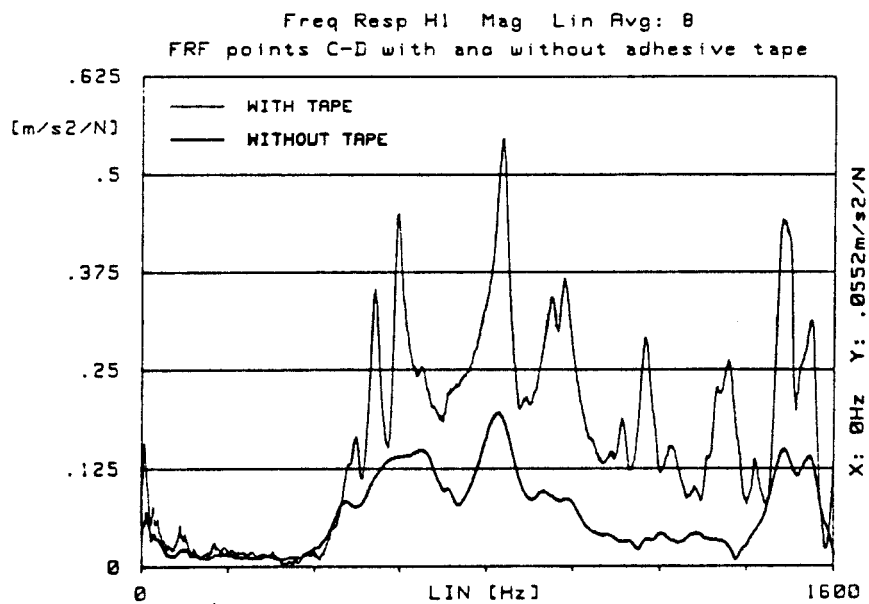by a vibrating plate.

Figure 7.   FRF between points C and D for plates (setups 3 and 4, with
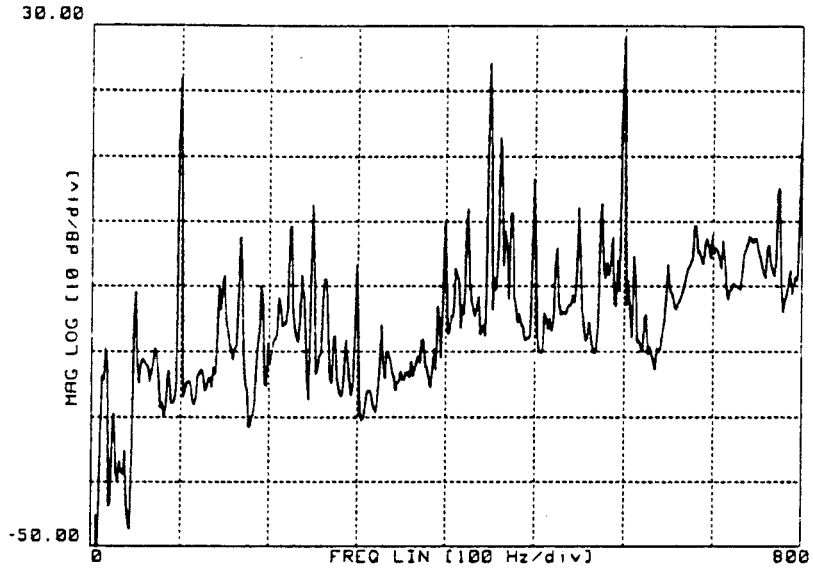and without tape).

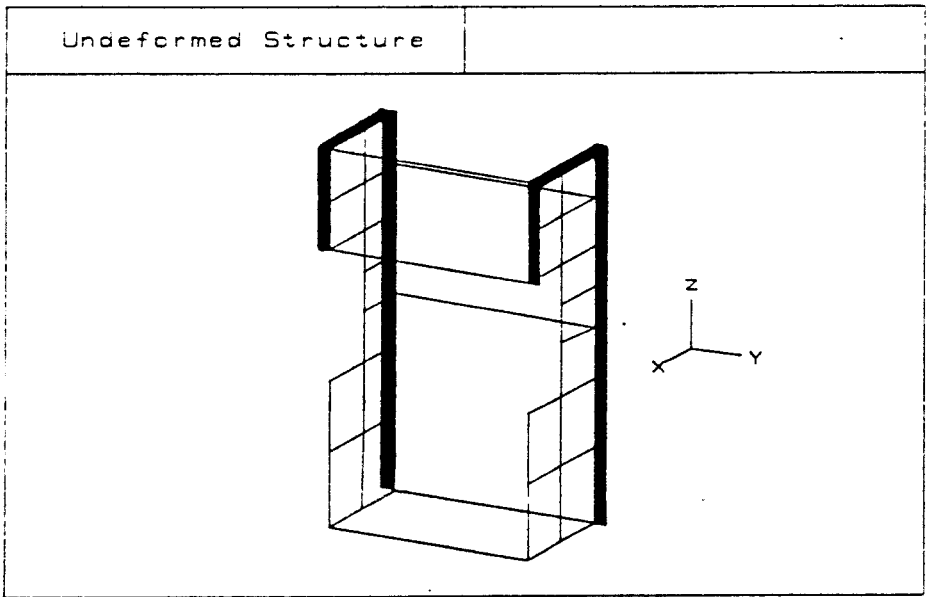Figure 8.   Spectrum of the force between DOFs 1Y and 15Y.

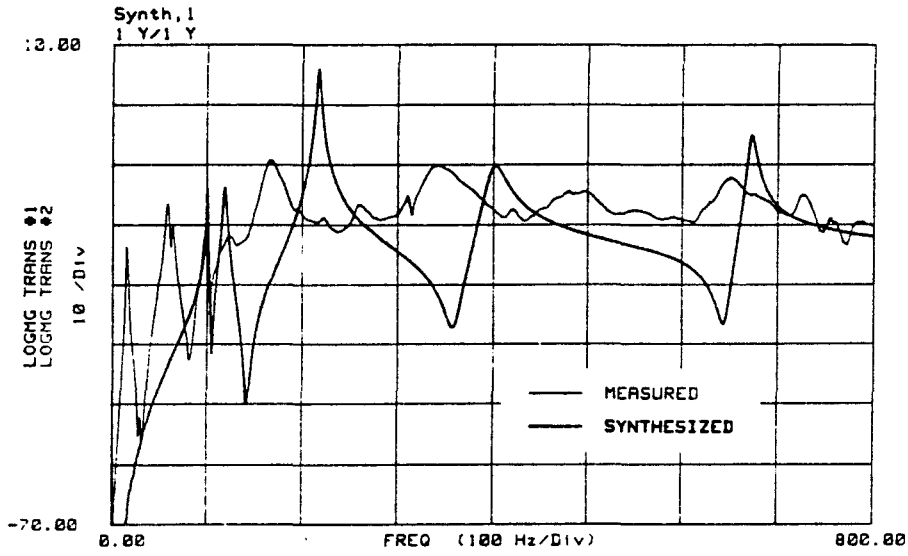Figure 9.   Structural modification: screw-on ribs.

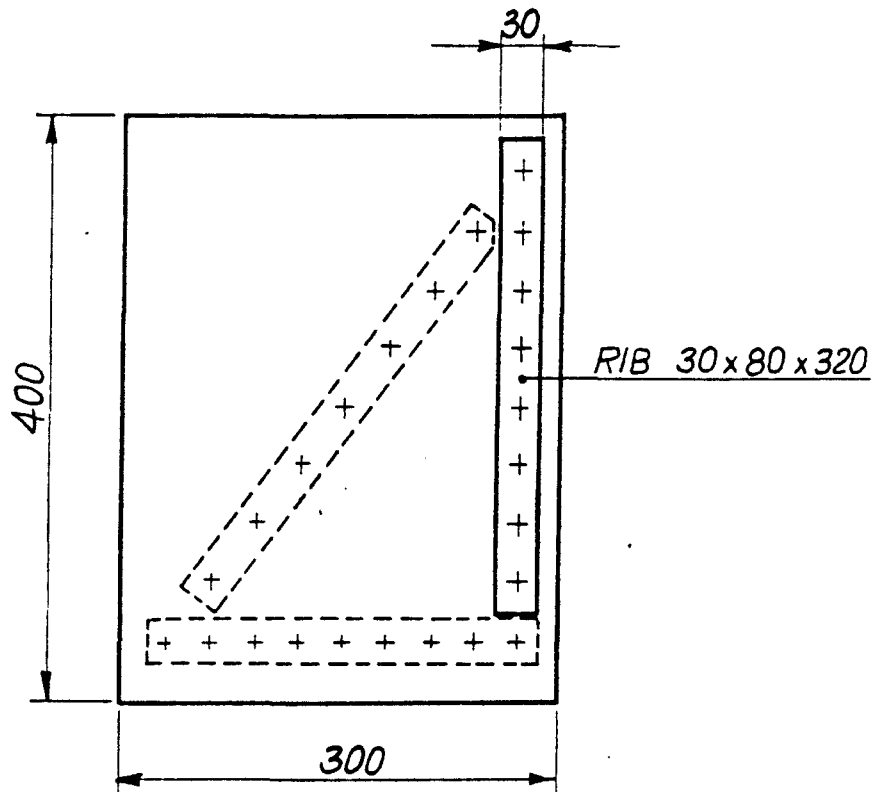Figure 10. FRF 1Y/1Y measured and synthesized.

Figure 11. Schematic of test model for verification of structural
modifications (screw-on ribs).